Handheld Burst Super-Resolution Meets Multi-Exposure Satellite Imagery

Jamy Lafenetre, Ngoc Long Nguyen, Gabriele Facciolo and Thomas Eboli

école normale supérieure paris—saclay

université PARIS-SACLAY

JUNE 18-22, 2023 CVPR VANCOUVER, CANADA

Context:

- ➢ Practical joint denoising and super-resolution based on multi-exposed satellite bursts.
- ➢ Interpretable, learning-free method based on adaptive kernel regression. No hallucinated details in the predictions.
- ➢ Robust to optical flow inaccuracies and off-model movements using a rejection mask.
- ➢ Considerably low-peak memory usage and runtime compared to SOTA deep learning.
- ➢ Robust to jitter on the reported exposure ratios.

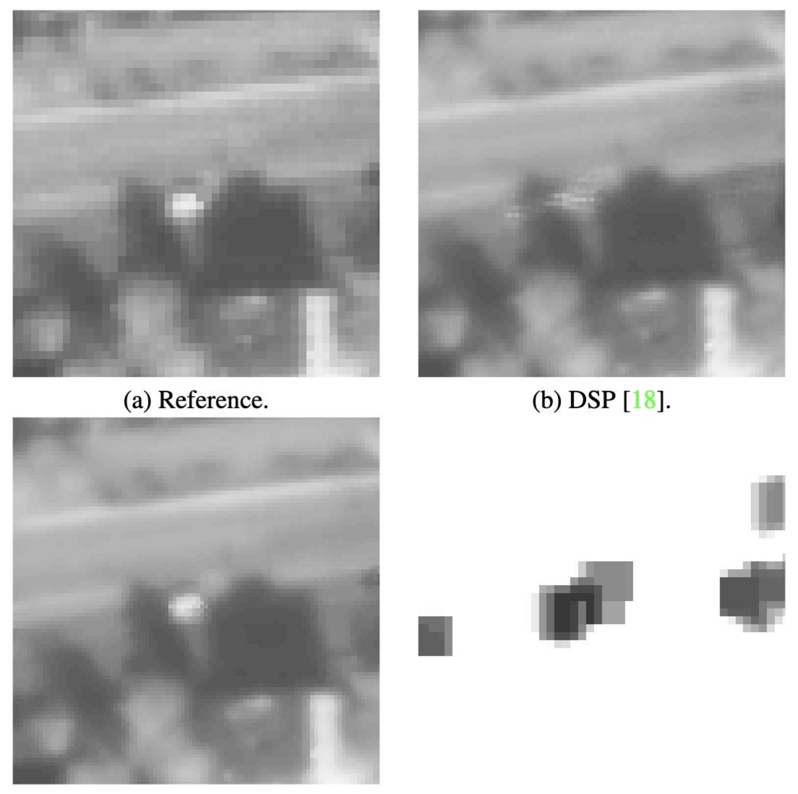

(a) Reference. (b) DSP [18]. (c) Ours. (d) Robustness mask.

Figure 5. Illustration of the robustness mask of our model on a set of real images. The white dot is a car moving forward on a road, and partially occluded by trees. The dark points on the accumulated robustness mask are areas where frames are rejected due to scene motion, and where the accumulation mostly relies on the reference frame.

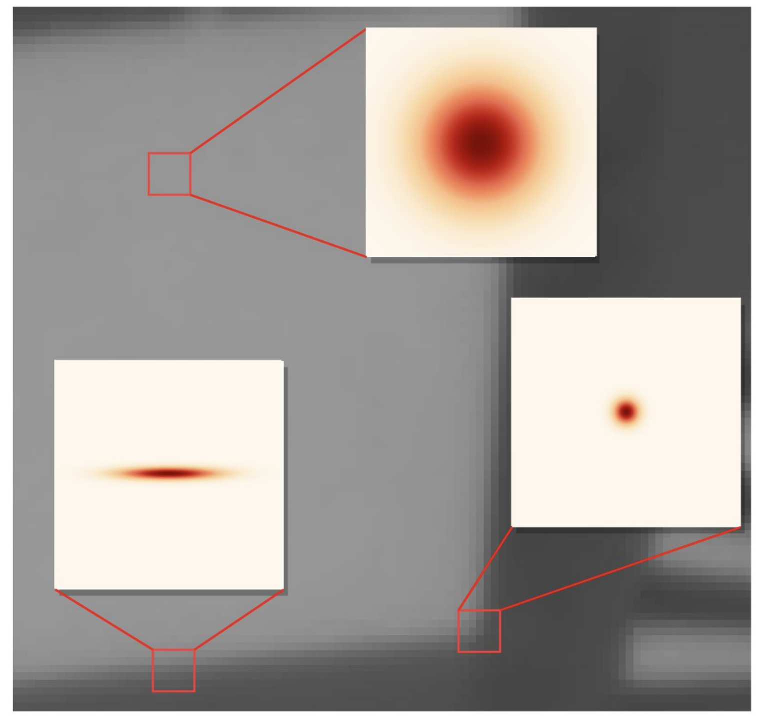

Figure 2. Illustration of the adaptive kernels of our method. A large isotropic kernel is used for areas without details, and a narrow isotropic kernel is used for areas such as corners. A stretched kernel is used for edges.

	Time (ms/burst)	Peak mem. (GB)
SA	49.5 ± 2.7	3.1
DSP [18]	548.3 ± 22.8	10.8
Ours (ICA)	129.7 ± 14.4	2.0
Ours (FNet)	118.6 ± 10.1	2.4

Table 5. Execution time per burst (s/burst) of size $15 \times 256 \times 256$ pixels on a single NVIDIA RTX 3090 graphic card. We benchmark our method for the patchwise ICA alignment, since an efficient GPU implementation had already been designed for [14], as well as with FNet flows.

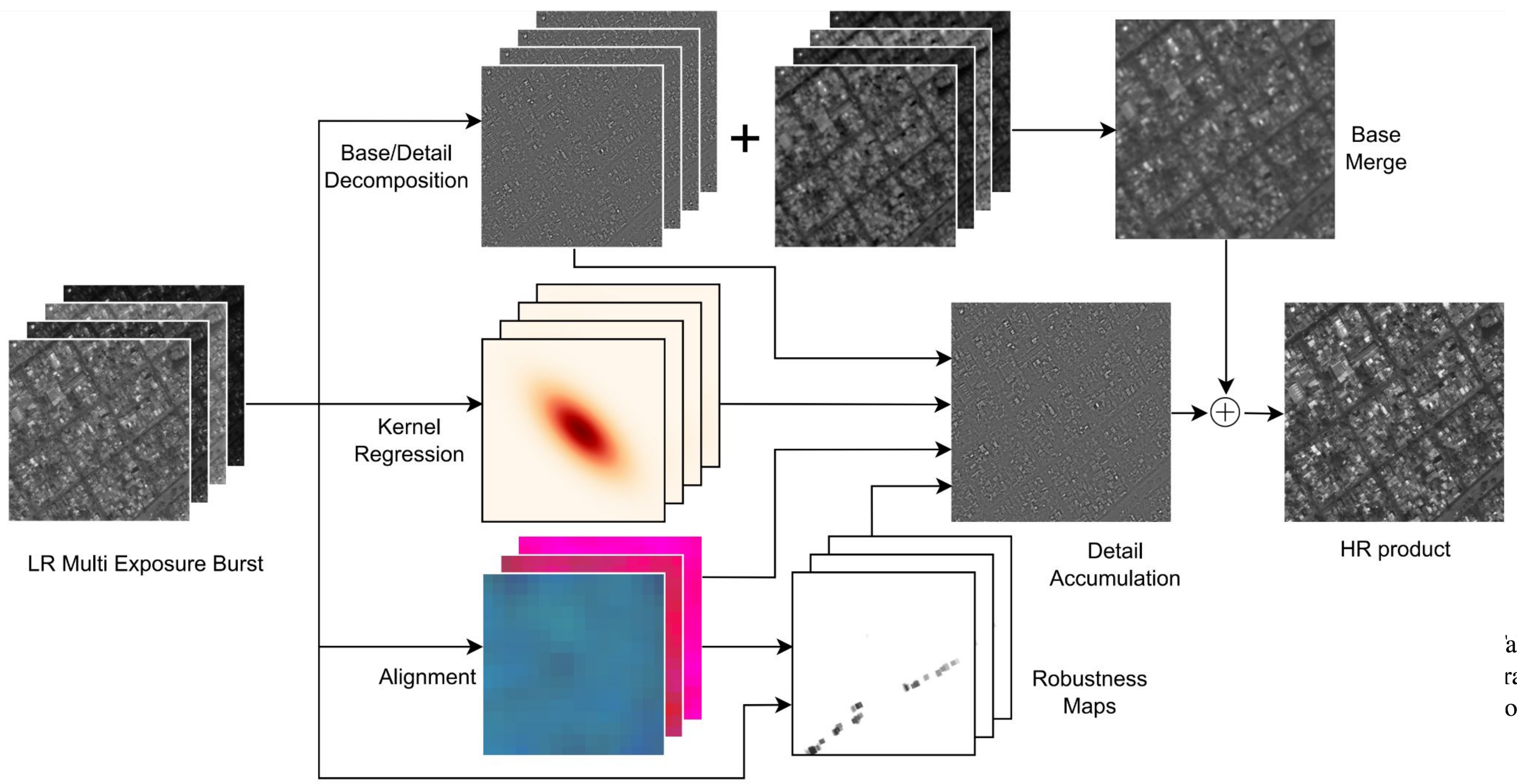

Handheld for Multi-Exposure Satellite Imagery:

- We generalize to satellite imagery the super-resolution algorithm of Wronski et. al, originally designed for handheld photography.
- The optical flow is model-agnostic: estimated using FNet or LK.
- Images are decomposed into base and detail components, to avoid artifacts caused by jitter on the exposure ratio.
- Details are merged using adaptive kernel regression:

$$D(x,y) = \frac{\sum_n \sum_{(p,q)\in\mathcal{N}} k_n(p,q) D_n(p,q)}{\sum_n \sum_{(p,q)\in\mathcal{N}} k_n(p,q)} \qquad w_n(x,y,u,v) = \exp\left(-\frac{1}{2} d^\top \Omega^{-1} d\right)$$

- Use anisotropic gaussian fusion weights adapted to the local geometry by leveraging the structure tensor.
- Potential misalignment and optical flow inaccuracies are detected and rejected by estimating interpretable robustness maps:

$$R(x,y) = \max\left(\min\left(s \times \exp\left(-\frac{d^2}{\sigma^2}\right) - t,\ 1\right),\ 0\right)$$

- The global shape of the kernel may be adjusted to the estimated SNR: joint denoising and SR.

Results:

- Despite running at a fraction of the cost of state-of-the-art algorithms, our approach perform almost as good for multi-exposed bursts.
- For single exposure bursts, our approach may perform better.
- The approach can automatically adjust to the estimated SNR.
- The approach never hallucinates, in contrast to DL methods.

	$N=5$	$N=10$	$N=15$
SA	49.14	51.83	53.11
ACTS [1]	48.88	51.64	52.93
DSP [18]	**51.21**	52.61	53.49
Ours	50.79	**52.74**	**53.78**

able 4. Single-exposure SR $\times 2$ with varying stack size N. Average PSNR on 200 bursts of size N varying in $\{5, 10, 15\}$, and oise of standard deviation of 16 DN.

	Exp. 0%	Exp. 5%	Exp. 20%
ACTS [1]	53.19	51.35	44.78
ACTS (B.D) [18]	52.79	52.71	50.97
SA	53.42	53.00	49.60
DSP [18]	**55.54**	**55.54**	**55.49**
Ours	54.53	52.98	46.07
Ours (B.D)	53.41	53.40	53.34

Table 6. Multi-exposure SR $\times 2$. Average PSNR on 200 bursts of $N = 15$ frames and exposure ratio jitter in $\{0, 5, 20\}$%.

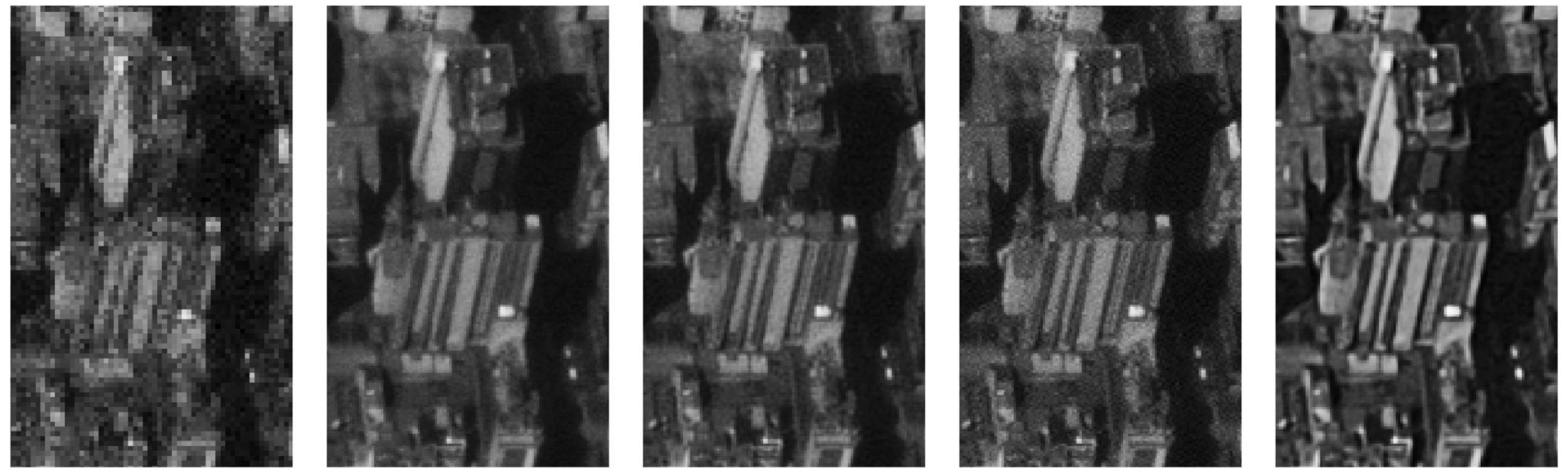

(a) Reference. (b) SA. (c) ACT [1]. (d) DSP [18]. (e) Ours.

Conclusion

- Interpretable lightweight joint multi-exposure SR alg.
- Results on par with recent CNNs but with less computes.

References

- Anger et al. Fast and Accurate Multi-Frame Super-Resolution of Satellite Images, ISPRS'20
- Lafenetre et al. Implementing Burst Super-Resolution, IPOL'23.
- Nguyen et al. Self-Supervised Multi-Image Super-Resolution for Push-Frame Satellite Images, EV'21
- Nguyen et al. Self-Supervised Super-Resolution for Multi-Exposure Push-Frame Satellites, CVPR'22.
- Wronski et al. Handheld Multi-Frame Super-Resolution, SIGGRAPH 2019